miR-20a-5p/RBM24 Axis Alleviated Hypertensive Intracerebral Hemorrhage via Regulating HIF1α/VEGFA Signaling Pathway

Li Xu
Nanjing Pukou Central Hospital
Chuangqi Mo
Nanjing Pukou Central Hospital
Ming Lu
Nanjing Pukou Central Hospital
Pingping Wang
Nanjing Pukou Central Hospital
Yue Liu (liuyue6283@163.com)
Nanjing Pukou Central Hospital

Research

Keywords: Hypertensive intracerebral hemorrhage, miR-20a-5p, RBM24, HIF1α/VEGFA signaling pathway

Posted Date: May 18th, 2021

DOI: https://doi.org/10.21203/rs.3.rs-520455/v1

Abstract

Background: Hypertensive intracerebral hemorrhage presented high incidence and high mortality owing to its difficult to diagnose. However, the molecular mechanism of HICH remains unclear. Therefore, this study aims to investigate the key miRNAs and the mechanism of the key miRNAs in HICH.

Methods: miRNAs chip was used to explore the differentially expressed miRNAs in HICH patients. In vitro and in vivo HICH models were established by Ang-II. Cell Counting Kit-8 (CCK8), flow cytometry, transwell assay and tube formation analysis were used to detect cell proliferation, apoptosis, cell migration and tube formation, respectively. Hematoxylin-eosin staining was used to evaluate the intracerebral hemorrhage in vivo HICH model. The regulatory mechanism of miR-20a-5p in HICH was confirmed by dual luciferase reporter assay, immunofluorescence, qRT-PCR, western blot and rescue experiments.

Results: miR-20a-5p showed the most downregulated in HICH patients compared with healthy individuals and significantly associated with clinicopathological characteristics of HICH. Upregulation of miR-20a-5p promoted cell proliferation, migration and tube formation while inhibited apoptosis in vitro and ameliorated the development of HICH in vivo. RBM24 is a direct target of miR-20a-5p and silencing RBM24 could partially recovery the development of HICH caused by miR-20a-5p inhibition both in vivo and in vitro. miR-20a-5p regulated the development of HICH depending on HIF1α/VEGFA pathway.

Conclusion: Our results demonstrated that miR-20a-5p/RBM24 axis regulated hypertensive intracerebral hemorrhage via regulating HIF1α/VEGFA signaling pathway, in support of further investigation into miR-20a-5p therapies for HICH treatment.

Introduction

Hypertensive cerebral hemorrhage (HICH) refers to the spontaneous hemorrhage in the brain parenchyma caused by hypertension or sudden increase in blood pressure [1, 2]. With the development of population aging, the incidence of HICH in our country is increasing year by year. So far, China has become one of the countries with high incidence of HICH in the world [3]. HICH has the characteristics of high disability and fatality rate, which brings a heavy burden to individuals, families and society. Although there are a variety of treatments in the pre-clinical field, many sequelae still occur, which affect the patient's ability of daily living and greatly reduce the patient's quality of life [4]. Therefore, it is of great significance to find effective molecular markers and study its molecular mechanism to provide more effective clinical treatments for HICH.

In recent years, with the development of medical imaging technology and the improvement of neurosurgery treatment, the disability and fatality rate of HICH has decreased, but the pathogenesis and the reasons for the high incidence of HICH are still not fully understood. The pathogenesis of HICH is relatively complex, involving multiple factors such as genetics, environment, infection, immunity, among which hypertension is the most important cause [5, 6]. Because intracranial arteries have the characteristics of less middle muscle cells and outer connective tissue, and lack of outer elastic layer,

long-term hypertension can cause hyalinosis, fibrinoid necrosis, and even the formation of microaneurysms or dissecting arteries. This will lead to the blood vessels rupture and cause bleeding when the blood pressure suddenly rises [7, 8]. With the rapid development of the advanced study in HICH, several molecular markers have been investigated on the incidence of HICH. Such as the COL1A2 rs42524 polymorphism was associated with the development of hypertensive intracerebral hemorrhage, particularly in conjunction with tobacco use and alcohol consumption in a Chinese population[9]. Recently, Liu et al., demonstrated that NIHSS score and high-density lipoprotein cholesterol level were prominently higher in HICH patients with CG and GG genotypes of ET-1 gene polymorphism rs1920453 than those in patients with CC genotype, suggesting that Rs1920453 in the promoter region of ET-1 gene was correlated with the occurrence of HICH [10]. However, there is still a lack of real targets for the diagnosis and treatment of HICH.

MicroRNAs (microRNAs, miRNAs) are endogenous non-coding single-stranded small RNAs with a length of 19–22 nucleotides, which are widely present in the biological world [11]. miRNAs regulate the expression of target genes by fully or partially complementary binding to the 3'UTR region of target mRNA[12] and participate in different physiological and pathological processes[13, 14]. Increasing numbers of studies have demonstrated that miRNAs play crucial roles in intracerebral hemorrhage by regulating various kinds of progresses [15]. For example, lncRNA Mtss1 promoted inflammatory responses and secondary brain injury after intracerebral hemorrhage by targeting miR-709 in mice [16]. Thrombin-induced miRNA-24-1-5p upregulation promoted angiogenesis by targeting prolyl hydroxylase domain 1 in intracerebral hemorrhagic rats [17]. For HICH, Dong et al., demonstrated that LncRNA-FENDRR mediated VEGFA to promote the apoptosis of brain microvascular endothelial cells via regulating miR-126 in mice with HICH [18], suggesting that miRNA might play crucial roles in HICH. However, it remains far from enough to discover key miRNAs in HICH, nor the mechanism. Therefore, in the present study, we intend to investigate the key miRNAs in the HICH and the mechanism of the miRNA involved in the development of HICH.

Materials And Methods

Clinical tissue collection

The human peripheral blood was collected from 60 HICH patients and healthy individuals who were admitted into the PuKou Branch Hospital of Jiangsu Province Hospital between 2017 and 2018. The diagnosis of HICH relies on CT imaging diagnosis and a history of hypertension. According to the results of CT examination and the bleeding site, HICH consists of basal ganglia, ventricular, thalamic, brainstem and cerebellar hemorrhage. The criteria that need to be excluded, including trauma, brain tumor, cerebral infarction, vascular malformation and secondary cerebral hemorrhage caused by other reasons. There was no significant difference between the two groups of patients’age, gender and other basic data after statistical analysis ($P > 0.05$). The experimental procedures were approved by the Ethics Committee of the PuKou Branch Hospital of Jiangsu Province Hospital, and written consents were obtained from each subject in advance.

RNA extraction and miRNA chip

The peripheral blood was collected from the HICH patients to perform miRNA chip, the healthy tissues act as control (N = 3). RNeasy Mini Kit (74104, QIAGEN) was used to isolate the RNA and RNA quantity and quality were measured by NanoDrop. Sample labeling and array hybridization were performed according to the Agilent miRNA Microarray Systemwith miRNA Complete Labeling and Hyb Kit protocol (Agilent Technology). After The hybridized arrays were washed, fixed and scanned with using the Agilent Microarray Scanner. Agilent Feature Extraction software (version 11.0.1.1) was used to analyze acquired array images. Quantile normalization and subsequent data processing were performed with using the GeneSpring GX v14.9 software package (Agilent Technologies). Differentially expressed miRNAs were identified through Fold Change filtering (Fold Change > 2.0, FDR < 1.0). R scripts was used to perform Hierarchical Clustering.

Hypertensive intracerebral hemorrhage model

Eight months old C57BL/6 mice were purchased from Charles River Laboratories (Beijing) to establish HICH model. The mice housed at room temperature (20–25°C) with a constant humidity (55 ± 5%) with free access to food and water at a regular 12/12-h light/dark cycle. The C57BL/6 mice were randomly divided into experimental and normal groups (n = 20). The experimental group was given angiotensin II (100mg/kg/day) in subcutaneously embedded micro-osmotic pump. Meanwhile, the mice were feed L-NAME L-NAME (100mg/kg/day) to construct a mouse model of hypertensive cerebral hemorrhage. The mice were fed normally for 18 weeks. Without act as control group. The HICH model was evaluated by blood pressure identification, behavioral testing and pathological testing. Blood pressure identification was measured by BP2000 sphygmomanometer; Behavioral tests were performed on the mice three times a day, including morning, middle and evening. When the contralateral forelimb stretched, hovered, trembling, or other motor dysfunction, it was regarded as a behavioral sign of cerebral hemorrhage in mice. The experiments involved animals were performed with the approval from the institutional animal care and the Ethics committee of the PuKou Branch Hospital of Jiangsu Province Hospital. For the function analysis of miR-20a-5p, 20 μg miR-20a-5p mimics or inhibitors were injected into mice via tail vein. For the function analysis of RBM24, lentivirus harboring the full length of RBM24 and sh-RNA sequence of RBM24 were injected into mice via tail vein, respectively.

Cell culture and treatment

Human umbilical vein endothelial cells (HUVECs) were purchased from The Global Bioresource Center (ATCC). After the HUVECs recovery, cells were cultured in the 90% Dulbecco's modified Eagle's medium (DMEM, 12430054, Gibco, USA) supplemented with 10% of fetal bovine serum (FBS, Gibco, USA), 100 U/mL penicillin and 100 μg/mL streptomycin at 37 ℃ in a 5% CO_2-contained incubator under 95% saturation humidity. HUVECs was induced for 12 hour by 1.00μmol/L AngII (Sigma) to establish HICH cell model. For function analysis of miR-20a-5p or RBM24, HUVECs were seeded in a six-well plate until the confluence reached at 70–90%. And then miR-20a-5p mimics or inhibitor, pCDNA-RBM24 or RBM24 SiRNA were transiently transfected into HUVECs and cultured for 24h, respectively. And then the cells

were used for further analysis. The miR-20a-5p mimics, inhibitor and NC sequences were synthesized by Shanghai GenePharma Co., Ltd. and sequences were listed as follows: miR-20a-5p mimics: 5'-UAAAGUGCUUAUAGUGCAGGUAGCUACCUGCACUAUAAGCACUUUA-3'; miR-20a-5p inhibitor: 5'-UAAAGUGCUGACAGUGCAGAU GCGAAGAGGTGACAGUGCAGA-3'; NC: 5'-GCACCGUCAAGGCUGAGAACUGGTGAAGACGCCAGUGGA-3'.

Luciferase assay

Fragments of RBM24 3'untranslated regions (UTR) including wild type (wt) or mutant (mt) miR-20a-5p binding sites were respectively inserted into the 3'-UTR of the luciferase reporter gene vector pmiGLO. The RBM24-wt or RBM24-mut pmiGLO vector were delivered into HEK293T cells by Lipofectamine® 3000 (Thermo Fisher) in the presence of miR-20a-5p mimic or inhibitor. The luciferase activity was determined using dual-luciferase reporter assay system kit (E1910, Promega, USA) according to the manufacturer's instruction. The luciferase activity was presented as firefly luciferase relative to that of renilla luciferase.

RNA extraction and quantification

Total RNA was extracted using the RNeasy Mini Kit (Qiagen, Valencia, CA, USA) according to the manufacturer's instruction. cDNA was synthesized from mRNA by using a HiScript II One Step RT-PCR Kit (Dye Plus) (P612-01, Vazyme, Nanjing, China) and miRNA 1st Strand cDNA Synthesis Kit (by stem-loop) (MR101-01, Vazyme, Nanjing, China) following the instructions which used for detecting the expression of RBM24, CTD, OPCML, HIF-α, VEGFA and miR-20a-5p following the instructions provided by the manufacturer's instruction. Real time quantitative PCR (qRT-qPCR) was performed with the ABI 7500 instrument (ABI, USA) RT-qPCR reaction mixture of volume 20 μL contained 9 μL of SYBR Mix, 0.5 μL of each primer (10 μM), 2 μL of the cDNA template, and 8 μL of RNase free H_2O. Thermal cycling parameters for the amplification were as follows: 95°C for 10 min, followed by 40 cycles at 95°C for 15 s, 60°C for 1 min. The miR-20a-5p level was normalized to U6 and the target mRNA level to GAPDH. Results were calculated by using $2^{-\triangle\triangle CT}$ method. The primers used in the present study was list as follows: miR-20a-5p Forward: 5'-TAAAGTGCTTATAGTGCAGGTAG-3', Reverse: 5'-GCAATGTAGAATCCGCTGGG-3'; U6 Forward: 5'-ACGCAAATTCGTGAAGCGTT-3', Reverse: 5'-CAGTCCAACTAGCACAATTCG-3'; GAPDH Forward 5'-GCACCGTCAAGGCTGAGAAC-3, Reverse: 5'-TGGTGAAGACGCCAGTGGA-3'.

Western blot

Total protein from HUVECs and brain tissues were extracted by using RIPA Lysis buffer. Protein abundances were determined using the BCA Protein Assay Kit (70-PQ0012, MultiSciences, China) following the manufacturer's instructions. 20 ug proteins for each sample with protein loading buffer were boiled at 100℃ for 5 min, followed by separation in 10–12% SDS-PAGE electrophoresis and transferred onto PVDF membranes. The membranes were then blocked with 5% lipid-free milk/TBST buffer for 2 h at room temperature, incubated with anti-RBM24, anti-HIF-1α antibody (ab51608, 1:2000), anti-VEGF-A antibody (ab183100, 1:450) and anti-GAPDH (ab8245, 1:5000, abcam, Cambridge, UK) primary antibodies for 2 h at 4℃overnight, respectively. After being incubation with secondary antibodies anti-mouse IgG (ab205719, 1:20000, abcam, Cambridge, UK) or anti-rabbit IgG (ab6721, 1:20000, abcam,

Cambridge, UK) for 1–2 h at room temperature, the immuno-complexes were finally detected by ECL after washing by TBST and analyzed using the Image-Pro Plus 6.0 software.

Cell proliferation, migration and tube formation analysis

The proliferation rates of cultured HUVECs with different treatments were measured by the Cell Counting 8 kit (#C0038; Beyotime) following the manufacturer's instruction. Briefly, HUVECs in were seeded in the 96-well plates, incubated with CCK-8 solution at 37°C for 24 h. Proliferation rates were finally evaluated by using microplate reader at 450 nm. For migration, Transwell chamber systems of 24-well plate with 8 μm wells were performed for cell migration assays. In brief, HUVECs were adjusted using the serum-free RPMI-1640 medium and 200 μL of cell suspension were added into the upper chambers. The cells that transferred to the lower chamber containing 10% FBS-supplemented DMEM (Invitrogen) incubation 24h at 37°Cwere subject to 4% paraformaldehyde fixation, 0.2% Triton X-100 treatment, and 0.05% crystal violet staining. For tube formation, HUVECs were plated in the plates coated by Matrigel (300 μL/well) at 3× 104 cells/well. The formation of vessels-like tube structures and migration were observed by using the inverted microscope (XDS-800D, Shanghai Caikang Optical Co. Ltd., China) and quantitated with Image J software.

Apoptosis analysis by TUNEL

Apoptosis analysis was performed by TUNEL analysis using a TUNEL detection kit (cat. no. KGA702; Nanjing KeyGen Biotech Co., Ltd.) according to the manufacturer's instructions. Briefly, $1x10^6$ cells were permeabilized with 0.1% Triton X-100 for 30 min and incubated in 50 mM TUNEL reaction mixture for 2 h at room temperature. In vivo apoptosis analysis, brain tissues slides were stained with 10 μl hematoxylin (cat. no. ab220365; Abcam) for 3 min at room temperature for nuclear staining. Images were captured using XSP-36 inverted fluorescence microscope (Boshida Optical Co., Ltd.). Each experiment was performed three times. Slides were counterstained with DAPI for 10 min at room temperature for nuclear staining. Images were captured using a fluorescence microscope (Olympus Corporation) and analyzed by image J.

Immunofluorescence staining

The expression and distribution of HIF-α and VEGFR were also detected by immunofluorescence in vivo and in vitro. In vitro, cells were seeded onto 12 mm coverslip in 24 well plates and cultured until their confluence reached about 70–80% and then fixed with 4% paraformaldehyde for 30 min at room temperature. The cells and the slides were blocked with 10% goat serum for 15 min followed by incubation with RBM24 (1:200, Abcam), HIFa (1:200, Abcam) or VEGFR primary antibodies overnight at 4ºC. The cells or slides were incubation with TRITC-conjugated or FITC-conjugated secondary antibody (Thermo Fisher, 1:200) for 1 hour at 37°C in the dark after washing with PBS and then counterstained with 4',6-diamidino-2-phenylindole (DAPI) (Sigma Aldrich, 0.1μg/ml) for 5 min. Images were taken using a fluorescent microscope.

Histopathological staining

Brain tissues from different groups were obtained and fixed with 4% paraformaldehyde followed by embedded in paraffin. Brain tissues were sliced into 4um sections for hematoxylin-eosin (HE) staining. Finally, the sections were rinsed and differentiated with 1% glacial acetic acid, and dehydrated in two tanks of absolute ethanol and dehydrate and sealed the slides with neutral gum. The tissue slices were taken by a microscope (Olympus, Japan).

Statistical analysis

All the statistical analyses in the present study were completed with SPSS 21.0 software (IBM, Armonk, NY, USA). Data are shown as the mean ± standard deviation with at least three independent experiments. Statistical comparisons were performed using unpaired t test between two groups and one-way analysis of variance (ANOVA) were used to compare more than two groups. Correlation of measurements was yielded with Pearson's correlation analysis. $P < 0.05$ was as a level of statistical significance.

Results

MicroRNA microarray profiling and differentially expressed miRNAs

Among the 2549 miRNAs tested using the Agilent 8 × 60 K miRNA-array platform, a total of 2134 miRNAs were found (Supplementary Table 1). Of them, a total of 715 miRNAs were found to be differentially expressed with 394 upregulation and 321 downregulation in the HICH patients compared to healthy individuals (Supplementary Table 2). And miR-20a-5p showed the most downregulated in HICH patients compared with healthy individuals (Fig. 1A). In order to confirm the results, the expression of miR-20a-5p were verified in HICH patients (n = 20) were by qRT-PCR. As shown in Fig. 1B, the expression of miR-20a-5p was significantly in HICH patients compared with healthy individuals. Therefore, miR-20a-5p was selected for further analysis.

miR-20a-5p is significantly associated with clinicopathological characteristics of HICH

We have demonstrated that miR-20a-5p was significantly in HICH patients compared with healthy individuals. In order to know whether miR-20a-5p participate in HICH, the correlation between miR-20a-5p expression and the clinicopathological characteristics of HICH was investigated. According to the expression of miR-20a-5p, 33 patients were divided into miR-20a-5p high expression group (n = 17) and low expression group (n = 16). The results showed the expression of miR-20a-5p was significantly correlated with higher cerebral hematoma volume, higher NIHSS index score and lower BI index score (Table 1).

Table 1
miR-20a-5p is significantly associated with clinicopathological characteristics of HICH

Group	Cases	Age	Sex	Cerebral hematoma volume(mL)	NIHSS index score	BI index score
High	17	60.24 ± 0.83	Female/male(9/8)	10.24 ± 1.24	8.34 ± 0.78	89.14 ± 6.83
Low	16	59.65 ± 0.72	Female/male(7/9)	18.34 ± 2.13	17.14 ± 2.83	72.67 ± 5.12
T value		0.176	0.243	7.9	6.87	
P value		0.845	0.971	< 0.001	< 0.001	< 0.001

miR-20a-5p regulated cell proliferation, apoptosis, migration and tube formation in vivo

In order to investigate the function of miR-20a-5p in HICH, the HICH model was established in HUVECs transfection with miR-20a-5p mimics or inhibitor. As shown in Fig. 2A-C, cell proliferation, migration and tube formation were significantly inhibited in miR-20a-5p inhibitor group while promoted in miR-20a-5p mimics group. Furthermore, apoptosis was dramatically increased in miR-20a-5p inhibitor group while decreased in miR-20a-5p mimics group (Fig. 2D). In addition, we found that the contents of HCy (homocysteine), ATII (angtiotensin□) and cTn I (cardiac troponin□) were significantly elevated in miR-20a-5p inhibitor group compared with miRNA-NC group while overexpression of miR-20a-5p decreased the contents of HCy, ATII and cTn I(Fig. 2E). These findings demonstrated that miR-195 plays an important role in cell proliferation, migration and tube formation of HUVECs.

Overexpression of miR-20a-5p inhibited HICH development in vivo

We have demonstrated that miR-20a-5p could regulate the development of HUVECs in vitro. Therefore, HICH model was constructed to confirm whether miR-20a-5p participated in the regulation of HICH in vivo. The blood pressure of the mice in the experimental group gradually increased and finally stabilized at about 180 mmHg while the blood pressure of the mice in the control group was stable at about 100 mm Hg (Fig. 3A). HE staining results showed that large bleeding area was observed in HICH rats (Fig. 3B), demonstrating the HICH was successfully established. Further analysis showed that the blood pressure was elevated when downregulation of miR-20a-5p while declined when overexpressing miR-20a-5p (Fig. 3C). The bleeding area was also sharply reduced in miR-20a-5p mimics group while increased in miR-20a-5p inhibitor group when compared with NC group (Fig. 3D). In addition, the contents of HCy, ATII and cTn I were significantly decreased in miR-20a-5p mimics group compared with miRNA-NC group while miR-20a-5p silencing increased the contents of HCy, ATII and cTn I (Fig. 3E).

RBM24 is a direct target of miR-20a-5p

In order to elucidate the underlying mechanism of miR-20a-5p involved in, the targets of miR-20a-5p were predicted by Targetscan7.2 (Supplementary Table 3). The expression of CTD (carboxy-terminal domain, RNA polymerase II, polypeptide A (CTD), small phosphatase-like opioid binding protein/cell adhesion molecule-like (OPCML) and RNA binding motif protein 24 (RBM24) which showed the highest cumulative weighted context + + score was measured by qRT-PCR and western blot. As shown in Fig. 4A and B, RBM24 showed the highest fold change and selected for further analysis. To confirm the relationship between miR-20a-5p and RBM24, a luciferase activity assay was conducted. As shown in Fig. 4C, the luciferase activity was significantly decreased in RBM24 WT group compared with control group while no obvious changes observed in RBM24 Mutant group compared with control group. In addition, the expression of RBM24 is significantly upregulated in HICH compared with healthy individuals. Further analysis showed that the expression of RBM24 is upregulated in miR-20a-5p inhibitor group while miR-20a-5p mimics could significantly attenuate the expression of RBM24 both in vitro and in vivo HICH models (Fig. 4D and E). These results indicated that RBM24 is a direct target of miR-20a-5p by binding its 3'UTR.

miR-20a-5p regulated the development of HICH by downregulation of RBM24

In order to know the function of RBM24 in the development of HICH, gain and loss function of RBM24 was performed in vivo and in vitro. In vitro experiments, we found that upregulation of RBM24 could inhibited cell proliferation, migration and tube formation while it could be promoted when downregulation of RBM24 (Fig. 5A-C). In addition, it showed that cell apoptosis was dramatically promoted in RBM24 overexpression group while inhibited in RBM24 suppression group (Fig. 5D). In vivo experiments, the blood pressure was elevated when upregulation of RBM24 while declined in suppressing RBM24 group (Fig. 5E). The bleeding area was also sharply increased in RBM24 overexpression group while reduced in RBM24 downregulation group compared with NC group (Fig. 5F). Furthermore, the contents of HCy, ATII and cTn I was significantly elevated in RBM24 upregulation group compared with miRNA-NC group while RBM24 suppressing decreased the contents of HCy, ATII and cTn I (Fig. 5G and H). In addition, the rescue experiment revealed that overexpression of RBM24 reversed the inhibitory effects of miR-20a-5p overexpression on the proliferation, migration, tube formation and apoptosis of HUVECs (Fig. 5I-L).

miR-20a-5p regulated the development of HICH depending on HIF1α/VEGFA pathway

It has been demonstrated that the HIF1α/VEGFA axis has been documented to be of great importance to angiogenesis. Therefore, we speculated that might by affecting HIF1α/VEGFA signaling pathways. To clarify whether HIF1α/VEGFA signaling pathway participated in the development of HICH depended on the miR-20a-5p-RBM24 axis, the expression of HIF1α and VEGFA was measured by qRT-PCR, western blot

and immunofluorescence staining. The results showed that the expression of HIF1α/VEGFA was significantly downregulated in HICH cells (Fig. 6A-C) and rats (Fig. 6D-F) compared with control group. Further analysis showed that overexpression of RBM24 could elevated the expression of HIF1α/VEGFA in HICH cells or rats (Fig. 6A-F), suggesting the effects of miR-20a-5p on the HIF-1α/VEGF-A pathway is dependent of RBM24.

Discussion

Surgical treatment alone cannot achieve satisfactory results to HICH due to the deep location of bleeding site in brain tissue. In view of the characteristics of rapid onset, high disability rate and high fatality rate, it brings a huge burden to individuals, families and society. Therefore, it is urgent to explore the effective biomarkers and in-depth study of their possible role in the pathogenesis, targeted therapy and prognosis of HICH. In the present study, we investigated the differentially expressed miRNAs in HICH. Of them, miR-20a-5p showed the most downregulated in HICH patients compared with healthy individuals and significantly associated with clinicopathological characteristics of HICH. Further analysis demonstrated that miR-20a-5p/RBM24 axis regulated hypertensive intracerebral hemorrhage via regulating HIF1α/VEGFA signaling pathway, in support of further investigation into miR-20a-5p therapies for HICH treatment. These results are of great significance for the diagnosis and treatment of HICH by miR-20a-5p.

Developmental defects in the middle layer of the arterial wall, arteriosclerosis and hypertension are three important factors for cerebral hemorrhage, among which hypertension is an important independent risk factor for cerebral hemorrhage [19]. Although the pathogenesis of HICH is not yet complete, it is currently believed that hypertension is an important basis for its pathogenesis, that is, hypertension induces mechanical stress changes to act on endothelial cells (ECs), causing a series of pathological changes, resulting in vascular wall damage [20]. However, the molecular mechanism of HICH is less studied. miRNA played an important role in a series of key biological processes, including cell proliferation, differentiation and metabolism [21]. Numbers of miRNAs have been revealed play crucial roles in intracerebral hemorrhage, such as miR-124, miR-340-5p and miR-26a-5p [22–24]. However, there was less studies focus on HICH regulated by miRNAs. In the present study, XX differentially expressed miRNAs in HICH patients were found by miRNAs chip. Of them, miR-20a-5p showed the most downregulated in HICH patients compared with healthy individuals and significantly associated with clinicopathological characteristics of HICH, demonstrating that miR-20a-5p played important roles in HICH. In fact, miR-20a-5p inhibited epithelial to mesenchymal transition and invasion of endometrial cancer cells by targeting STAT3 [25]. Recently, it demonstrated that MicroRNA-20a-5p suppressed tumor angiogenesis of non-small cell lung cancer through RRM2-mediated PI3K/Akt signaling pathway [26]. In the present study, we found that downregulation of miR-20a-5p promoted cell proliferation, migration and tube formation while inhibited apoptosis in vitro and ameliorated the development of HICH in vivo. These results demonstrated that miR-20a-5p regulated the development of HICH by regulating the angiogenesis.

miRNA could inhibit the mRNA expression by binding the 3’UTR of its targets in various kinds of diseases. In the present study, we found that RBM24 is a direct target of miR-20a-5p. It has been demonstrated that

RBM24 played important roles in many progresses of various diseases, such as cell alternative splicing, lung cancer progression and skeletal muscle regeneration [27, 28]. In addition, it also proved that RBM24 could regulated by miRNAs. For example, MicroRNA-222 regulates muscle alternative splicing through Rbm24 during differentiation of skeletal muscle cell [29]; The restoration of RBM24 expression suppressed NPC cellular proliferation, migration and invasion and impeded metastatic colonization in mouse models by upregulating miR-25[30]. However, the function of RBM24 remains unclear in HICH. In the present study, we showed that overexpression of RBM24 inhibited the cell proliferation, migration and tube formation while promoted apoptosis in vitro and ameliorated the development of HICH in vivo. Further analysis showed that silencing RBM24 could partially recovery the development of HICH caused by miR-20a-5p inhibition both in vivo and in vitro. These results demonstrated that miR-20a-5p regulated the development of HICH via regulating the expression of RBM24.

The HIF1α/VEGFA axis has been documented to be of great importance to angiogenesis in multiple diseases [31–33], as well as in intracerebral hemorrhage. Such as HIF-1α gene can promote the proliferation, migration and differentiation of endogenous neural stem cells after ICH, thereby contributing to neurofunctional recovery after ICH [34]. It also proved that HIF-1α and downstream pathways could regulate neuronal injury after intracerebral hemorrhage in diabetes [35]. Recently, Cui et al., demonstrated that thrombin reduced HIF-1α degradation and initiated angiogenesis by increasing miR-24, which targets PHD1 after ICH, suggesting HIF-1α might involve in the regulation of HICH [17]. In the present study, we demonstrated that the expression of HIF1α/VEGFA was significantly downregulated in HICH cells and rats compared with control group. Further analysis showed that overexpression of RBM24 could inhibit the expression of HIF1α/VEGFA while siRNA knockdown of RBM24 reversed the changes, suggesting the effects of miR-20a-5p on the HIF-1α/VEGF-A pathway is dependent of RBM24. Taken together, our results demonstrate miR-20a-5p/RBM24 axis regulated hypertensive intracerebral hemorrhage via regulating HIF1α/VEGFA signaling pathway, in support of further investigation into miR-20a-5p therapies for HICH treatment.

In summary, we found that miR-20a-5p showed the most downregulated in HICH patients compared with healthy individuals and significantly associated with clinicopathological characteristics of HICH. Further analysis showed that miR-20a-5p/RBM24 axis regulated hypertensive intracerebral hemorrhage via regulating HIF1α/VEGFA signaling pathway. These findings will provide solid foundation to prevent the occurrence and development of HICH.

Declarations

Ethics approval and consent to participate

The experimental procedures were approved by the Ethics Committee of the PuKou Branch Hospital of Jiangsu Province Hospital, and written consents were obtained from each subject in advance. The contents of this study are under full compliance with government policy and the Declaration of Helsinki.

Consent for publication

Not applicable.

Availability of data and materials

The datasets during and/or analyzed during the current study available from the corresponding author on reasonable request.

Competing interests

The authors declare that they have no competing interests.

Acknowledgement and Funding

This work was supported by the Pukou district social science and technology planning project of 2018 (s2018-05) and Science and Technology Development Fund of Pukou Branch Hospital of Jiangsu Province Hospital (KJ2021-7).

Authors' contributions

Li Xu performed experiments and wrote the manuscript. Li Xu, Chuangqi Mo, Ming Lu and Pingping Wang performed experiments and analyzed data. Yue Liu supervised this project and revised the manuscript. All authors read and approved the final manuscript.

References

1. Ueno M: [Hypertensive cerebral hemorrhage]. Nihon rinsho Japanese journal of clinical medicine 2004, 62 Suppl 3:363-368.
2. Fisher CM: Hypertensive cerebral hemorrhage. Demonstration of the source of bleeding. Journal of neuropathology and experimental neurology 2003, 62(1):104-107.
3. Ziai WC, Thompson CB, Mayo S, McBee N, Freeman WD, Dlugash R, Ullman N, Hao Y, Lane K, Awad I et al: Intracranial Hypertension and Cerebral Perfusion Pressure Insults in Adult Hypertensive Intraventricular Hemorrhage: Occurrence and Associations With Outcome. Critical care medicine 2019, 47(8):1125-1134.
4. Ding W, Gu Z, Song D, Liu J, Zheng G, Tu C: Development and validation of the hypertensive intracerebral hemorrhage prognosis models. Medicine 2018, 97(39):e12446.
5. Gavito-Higuera J, Khatri R, Qureshi IA, Maud A, Rodriguez GJ: Aggressive blood pressure treatment of hypertensive intracerebral hemorrhage may lead to global cerebral hypoperfusion: Case report and imaging perspective. World journal of radiology 2017, 9(12):448-453.
6. Che XR, Wang YJ, Zheng HY: Prognostic value of intracranial pressure monitoring for the management of hypertensive intracerebral hemorrhage following minimally invasive surgery. World journal of emergency medicine 2020, 11(3):169-173.

7. Zia E, Hedblad B, Pessah-Rasmussen H, Berglund G, Janzon L, Engstrom G: Blood pressure in relation to the incidence of cerebral infarction and intracerebral hemorrhage. Hypertensive hemorrhage: debated nomenclature is still relevant. Stroke 2007, 38(10):2681-2685.
8. Lei C, Wu B, Liu M, Cao T, Wang Q, Dong W: Differences Between Vascular Structural Abnormality and Hypertensive Intracerebral Hemorrhage. Journal of stroke and cerebrovascular diseases : the official journal of National Stroke Association 2015, 24(8):1811-1816.
9. Tian DZ, Wei W, Dong YJ: Influence of COL1A2 gene variants on the incidence of hypertensive intracerebral hemorrhage in a Chinese population. Genetics and molecular research : GMR 2016, 15(1).
10. Liu J, Gao DY, Li JN: Correlations of endothelin-1 gene polymorphisms and hypertensive intracerebral hemorrhage. European review for medical and pharmacological sciences 2020, 24(22):11776-11782.
11. Mendell JT: MicroRNAs: critical regulators of development, cellular physiology and malignancy. Cell cycle 2005, 4(9):1179-1184.
12. Bartel DP: MicroRNAs: genomics, biogenesis, mechanism, and function. Cell 2004, 116(2):281-297.
13. Weldon Furr J, Morales-Scheihing D, Manwani B, Lee J, McCullough LD: Cerebral Amyloid Angiopathy, Alzheimer's Disease and MicroRNA: miRNA as Diagnostic Biomarkers and Potential Therapeutic Targets. Neuromolecular medicine 2019, 21(4):369-390.
14. Gareev IF, Safin SM: [The role of endogenous miRNAs in the development of cerebral aneurysms]. Zhurnal voprosy neirokhirurgii imeni N N Burdenko 2019, 83(1):112-118.
15. Li L, Wang P, Zhao H, Luo Y: Noncoding RNAs and Intracerebral Hemorrhage. CNS & neurological disorders drug targets 2019, 18(3):205-211.
16. Chen JX, Wang YP, Zhang X, Li GX, Zheng K, Duan CZ: lncRNA Mtss1 promotes inflammatory responses and secondary brain injury after intracerebral hemorrhage by targeting miR-709 in mice. Brain research bulletin 2020, 162:20-29.
17. Cui H, Yang A, Zhou H, Wang Y, Luo J, Zhou J, Liu T, Li P, Zhou J, Hu E et al: Thrombin-induced miRNA-24-1-5p upregulation promotes angiogenesis by targeting prolyl hydroxylase domain 1 in intracerebral hemorrhagic rats. Journal of neurosurgery 2020:1-12.
18. Dong B, Zhou B, Sun Z, Huang S, Han L, Nie H, Chen G, Liu S, Zhang Y, Bao N et al: LncRNA-FENDRR mediates VEGFA to promote the apoptosis of brain microvascular endothelial cells via regulating miR-126 in mice with hypertensive intracerebral hemorrhage. Microcirculation 2018, 25(8):e12499.
19. Ishisaka T, Igarashi Y, Kodera K, Okuno T, Morita T, Himeno T, Hamada K, Yano H, Higashikawa T, Iritani O et al: Relationship Between Blood Pressure Levels on Admission and the Onset of Acute Pneumonia in Elderly Patients With Cerebral Hemorrhage. Journal of clinical medicine research 2020, 12(11):693-698.
20. Pasi M, Sugita L, Xiong L, Charidimou A, Boulouis G, Pongpitakmetha T, Singh S, Kourkoulis C, Schwab K, Greenberg SM et al: Association of cerebral small vessel disease and cognitive decline after intracerebral hemorrhage. Neurology 2020.

21. Grillari J, Makitie RE, Kocijan R, Haschka J, Vazquez DC, Semmelrock E, Hackl M: Circulating miRNAs in bone health and disease. Bone 2020:115787.
22. Bao WD, Zhou XT, Zhou LT, Wang F, Yin X, Lu Y, Zhu LQ, Liu D: Targeting miR-124/Ferroportin signaling ameliorated neuronal cell death through inhibiting apoptosis and ferroptosis in aged intracerebral hemorrhage murine model. Aging cell 2020, 19(11):e13235.
23. Zhou W, Huang G, Ye J, Jiang J, Xu Q: Protective Effect of miR-340-5p against Brain Injury after Intracerebral Hemorrhage by Targeting PDCD4. Cerebrovascular diseases 2020, 49(6):593-600.
24. Zhang H, Lu X, Hao Y, Tang L, He Z: MicroRNA-26a-5p alleviates neuronal apoptosis and brain injury in intracerebral hemorrhage by targeting RAN binding protein 9. Acta histochemica 2020, 122(5):151571.
25. Huang Y, Yang N: MicroRNA-20a-5p inhibits epithelial to mesenchymal transition and invasion of endometrial cancer cells by targeting STAT3. International journal of clinical and experimental pathology 2018, 11(12):5715-5724.
26. Han J, Hu J, Sun F, Bian H, Tang B, Fang X: MicroRNA-20a-5p suppresses tumor angiogenesis of non-small cell lung cancer through RRM2-mediated PI3K/Akt signaling pathway. Molecular and cellular biochemistry 2020.
27. Zhang D, Ma Y, Ma Z, Liu S, Sun L, Li J, Zhao F, Li Y, Zhang J, Li S et al: Circular RNA SMARCA5 suppressed non-small cell lung cancer progression by regulating miR-670-5p/RBM24 axis. Acta biochimica et biophysica Sinica 2020, 52(10):1071-1080.
28. Zhang M, Han Y, Liu J, Liu L, Zheng L, Chen Y, Xia R, Yao D, Cai X, Xu X: Rbm24 modulates adult skeletal muscle regeneration via regulation of alternative splicing. Theranostics 2020, 10(24):11159-11177.
29. Cardinali B, Cappella M, Provenzano C, Garcia-Manteiga JM, Lazarevic D, Cittaro D, Martelli F, Falcone G: MicroRNA-222 regulates muscle alternative splicing through Rbm24 during differentiation of skeletal muscle cells. Cell death & disease 2016, 7:e2086.
30. Hua WF, Zhong Q, Xia TL, Chen Q, Zhang MY, Zhou AJ, Tu ZW, Qu C, Li MZ, Xia YF et al: RBM24 suppresses cancer progression by upregulating miR-25 to target MALAT1 in nasopharyngeal carcinoma. Cell death & disease 2016, 7(9):e2352.
31. Wan J, Wu W, Chen Y, Kang N, Zhang R: Insufficient radiofrequency ablation promotes the growth of non-small cell lung cancer cells through PI3K/Akt/HIF-1alpha signals. Acta biochimica et biophysica Sinica 2016, 48(4):371-377.
32. Liang H, Xiao J, Zhou Z, Wu J, Ge F, Li Z, Zhang H, Sun J, Li F, Liu R et al: Hypoxia induces miR-153 through the IRE1alpha-XBP1 pathway to fine tune the HIF1alpha/VEGFA axis in breast cancer angiogenesis. Oncogene 2018, 37(15):1961-1975.
33. Wang J, Man GCW, Chan TH, Kwong J, Wang CC: A prodrug of green tea polyphenol (-)-epigallocatechin-3-gallate (Pro-EGCG) serves as a novel angiogenesis inhibitor in endometrial cancer. Cancer letters 2018, 412:10-20.

34. Yu Z, Chen LF, Tang L, Hu CL: Effects of recombinant adenovirus-mediated hypoxia-inducible factor-1alpha gene on proliferation and differentiation of endogenous neural stem cells in rats following intracerebral hemorrhage. Asian Pacific journal of tropical medicine 2013, 6(10):762-767.
35. Yu Z, Tang L, Chen L, Li J, Wu W, Hu C: Role for HIF-1alpha and Downstream Pathways in Regulating Neuronal Injury after Intracerebral Hemorrhage in Diabetes. Cellular physiology and biochemistry : international journal of experimental cellular physiology, biochemistry, and pharmacology 2015, 37(1):67-76.

Figures

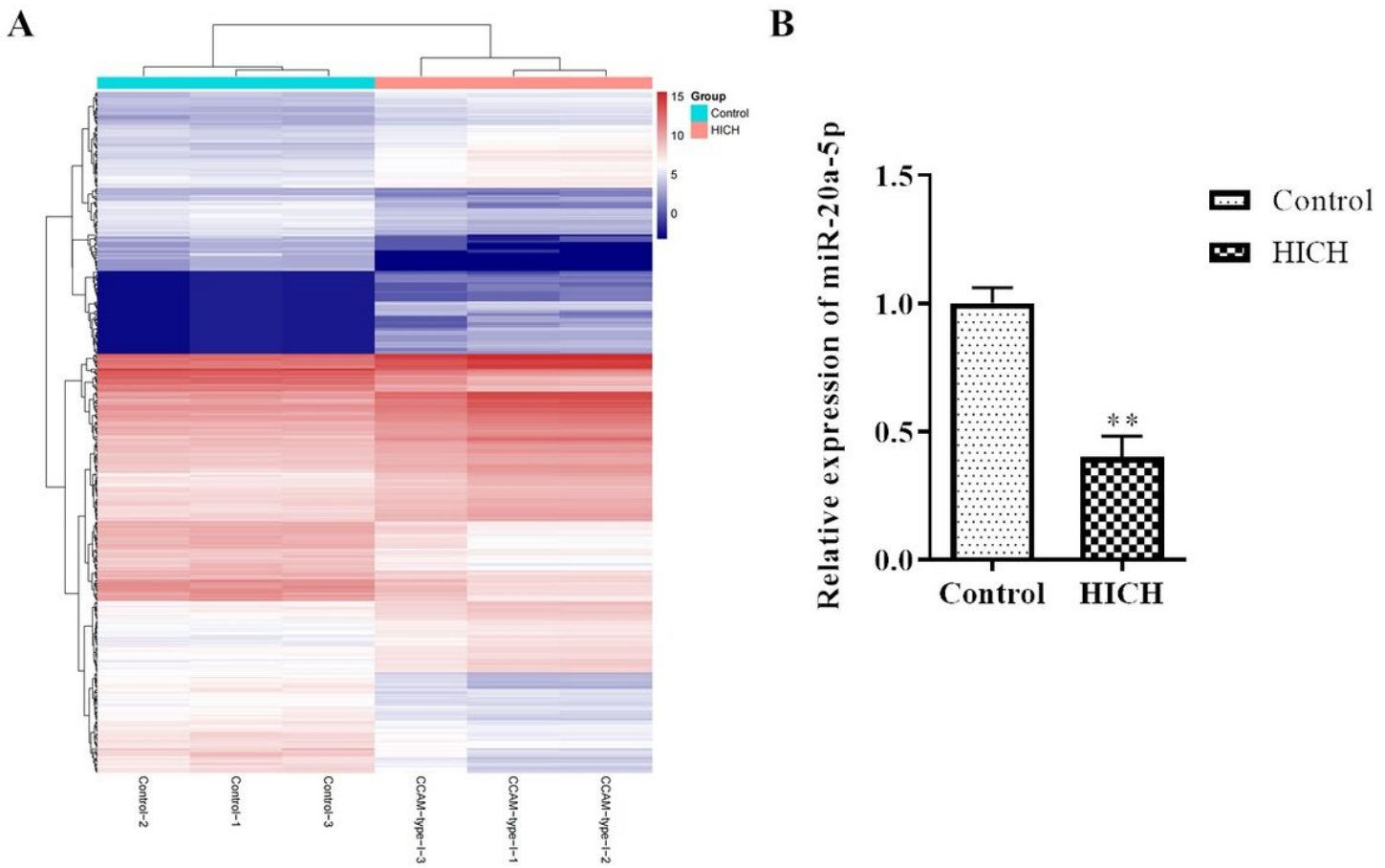

Figure 1

MicroRNA microarray profiling and differentially expressed miRNAs. (A) Heatmap present the differentially expressed miRNA in the HICH patients. (B) qRT-PCR analysis to miR-20a-5p in the HICH patients and control group. U6 act as control. *P < 0.05. All data are expressed as the mean ± SD.

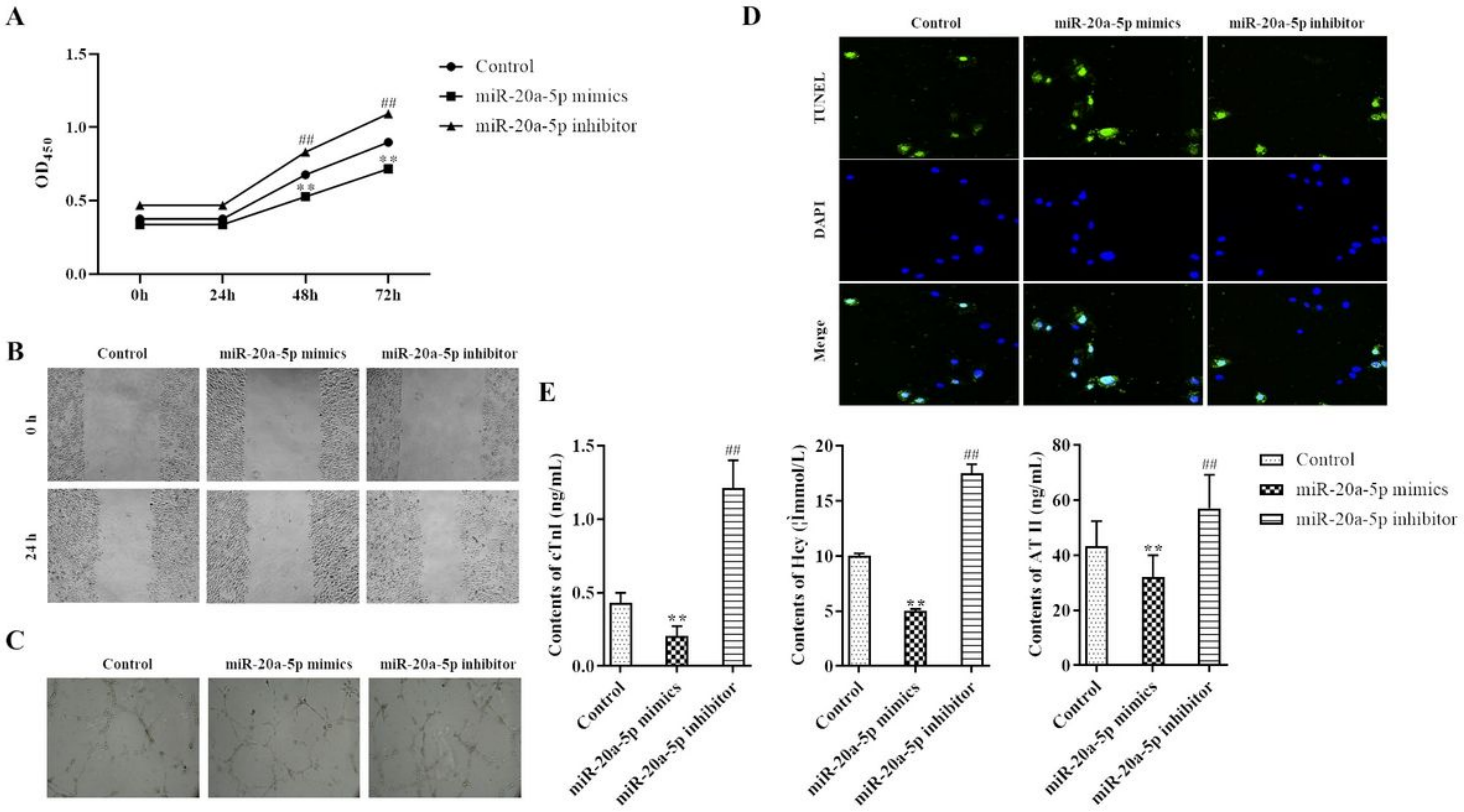

Figure 2

miR-20a-5p regulated cell proliferation, apoptosis, migration and tube formation in vitro. (A) Cell proliferation was analyzed by CCK-8. (B) Migration was detected by transwelll analysis. (C) Tube formation analysis to detect the tube formation treatment with miR-20a-5p inhibitor or miR-20a-5p mimics. (D) Apoptosis was measured by Flow cytometer. (E) The contents of HCy, ATII and cTn I detected by ELISA. *p < 0.05. All data are expressed as the mean ± SD.

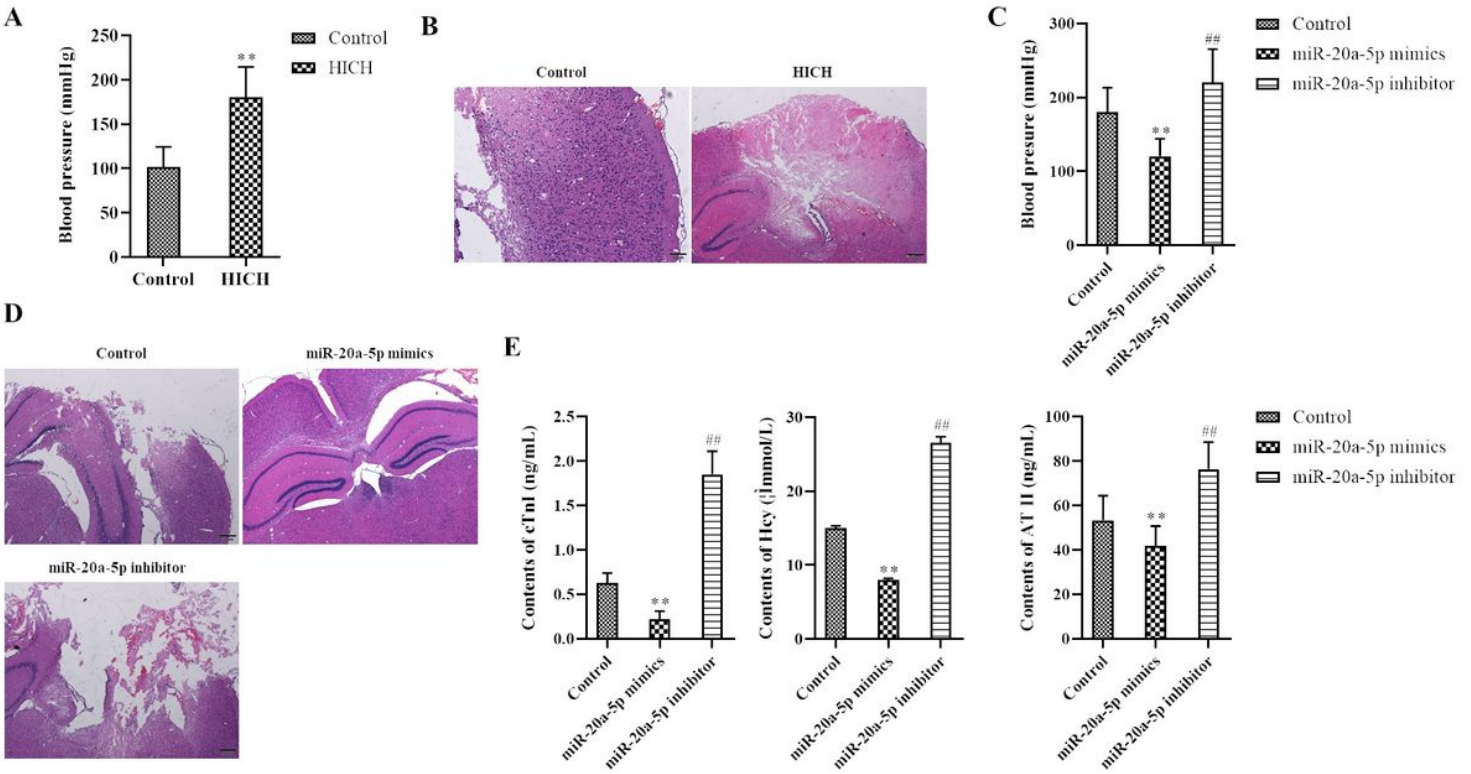

Figure 3

miR-20a-5p regulate development of HICH in vivo. (A) Blood pressure in HICH and contro groups. (B) HE analysis to bleeding area in HICH rats. (C) Blood pressure in HICH and control groups when overexpressing or silencing miR-20a-5p. (D) HE analysis to bleeding area in HE analysis to bleeding area in overexpressing or silencing miR-20a-5p HICH rats. (E) The contents of HCy, ATII and cTn I detected by ELISA in overexpressing or silencing miR-20a-5p HICH rats. *p < 0.05. All data are expressed as the mean ± SD.

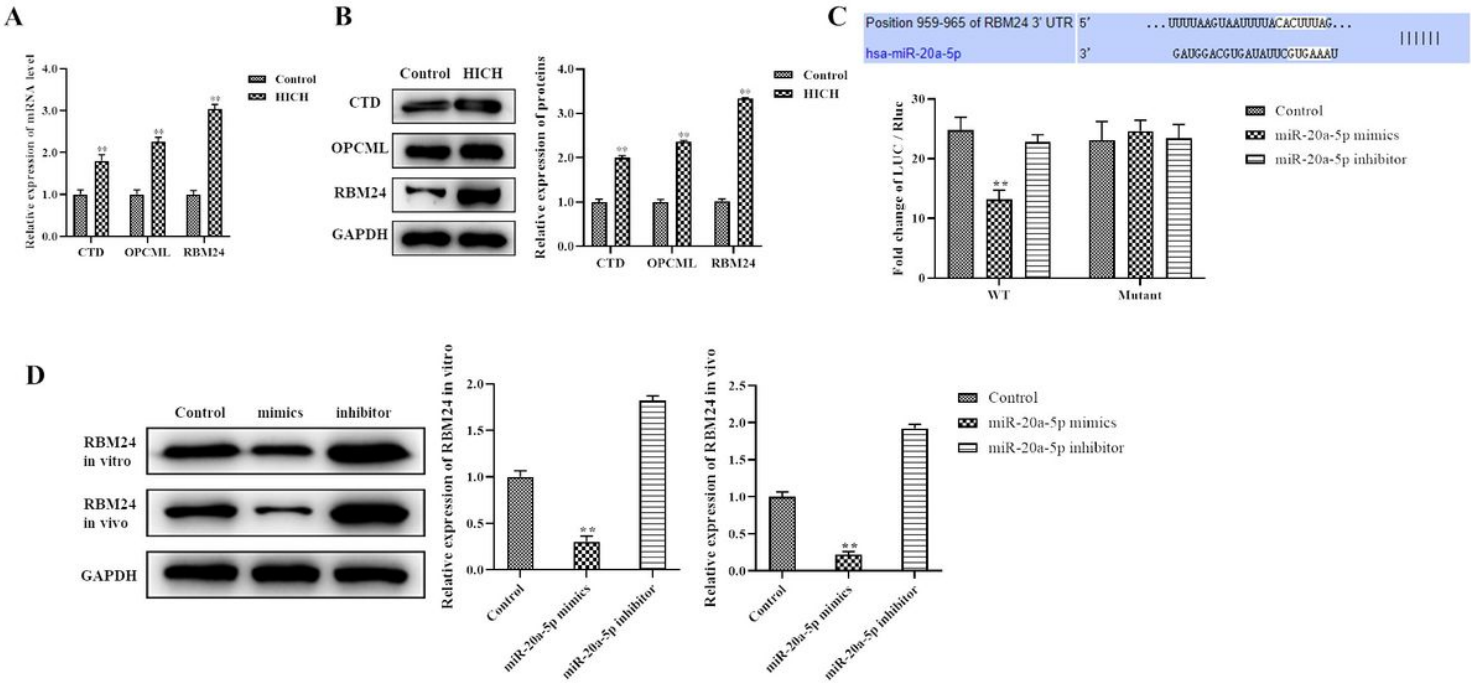

Figure 4

RMB24 is a direct target of miR-20a-5p. (A-B) The expression of CTD, OPCML and RBM24 detected by qRT-PCR and Western blot. (C) Dual luciferase reporter analysis to RMB24 regulated by miR-20a-5p. (D-E) The expression levels of RMB24 protein after treatment with miR-20a-5p mimics, miR-20a-5p inhibitor or miR NC in vitro and in vivo, respectively. GAPDH act as control. **P<0.05, All data are expressed as the mean ± SD.

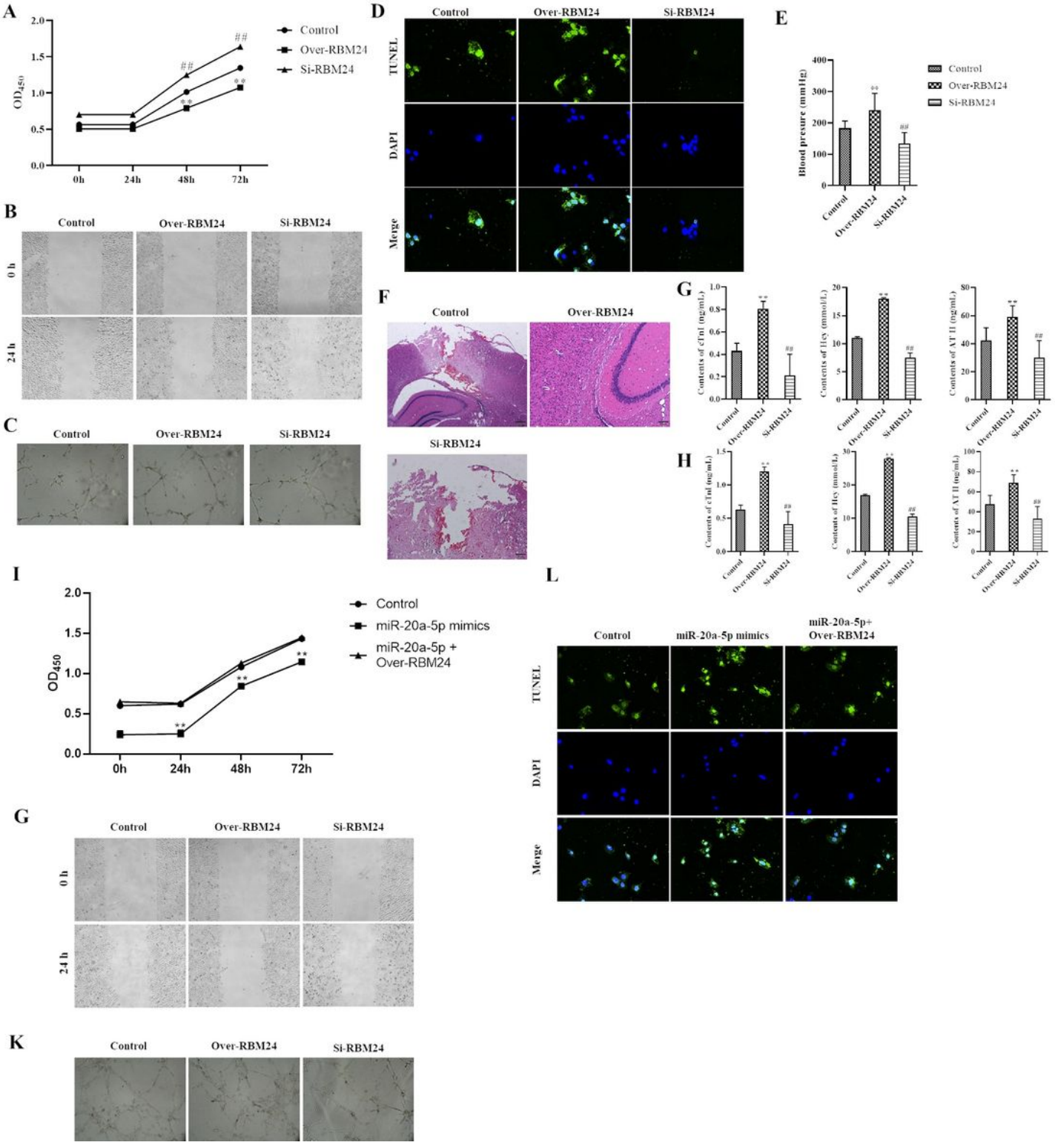

Figure 5

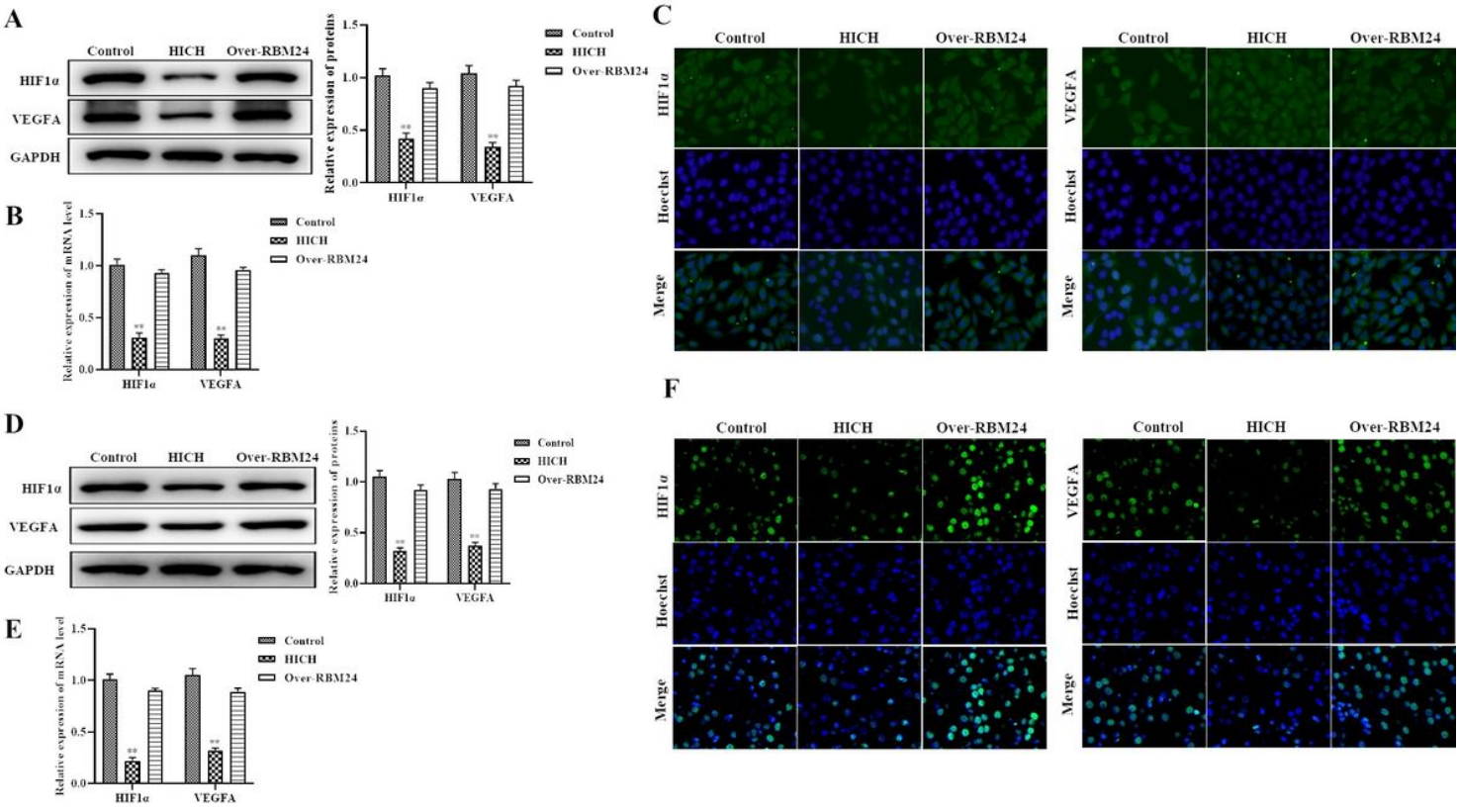

Figure 6

miR-20a-5p regulated the development of HICH by downregulation of RBM24. (A) Cell proliferation was analyzed by CCK-8 in overexpressing or silencing RBM24 in vitro. (B) Migration was detected by transwelll analysis in overexpressing or silencing RBM24 in vitro. (C) Tube formation analysis to detect the tube formation in overexpressing or silencing RBM24 in vitro. (D) Apoptosis was measured by TUNEL analysis in overexpressing or silencing RBM24 in vitro. (E) Blood pressure in HICH and control groups when overexpressing or silencing RBM24. (F) HE analysis to bleeding area in HE analysis to bleeding area in overexpressing or silencing RBM24. (G-H) The contents of HCy, ATII and cTn I detected by ELISA in overexpressing or silencing RBM24 HICH rats. (I) Cell proliferation was analyzed by CCK-8 in miR-20a-5p mimics group rescued by overexpressing RBM24 in vitro. (G) Migration was detected by transwelll analysis in in miR-20a-5p mimics group rescued by overexpressing RBM24 in vitro. (K) Tube formation analysis to detect the tube formation in in miR-20a-5p mimics group rescued by overexpressing RBM24 in vitro. (L) Apoptosis was measured by TUNEL analysis in miR-20a-5p mimics group rescued by overexpressing RBM24 in vitro. *p < 0.05. All data are expressed as the mean ± SD.

Figure 6

miR-20a-5p regulated the development of HICH depending on HIF1α/VEGFA pathway. (A-C) The expression of HIF1α and VEGFA was measured by qRT-PCR, western blot and immunofluorescence staining after RBM24 overexpression or suppression in cells, respectively. (D-F) The expression of HIF1α and VEGFA was measured by qRT-PCR, western blot and immunofluorescence staining after RBM24 overexpression or suppression in HICH rats, respectively GAPDH act as control for qRT-PCR and western

blot. The relative grey density was calculated by Image J. *p < 0.05. All data are expressed as the mean ± SD.

Supplementary Files

This is a list of supplementary files associated with this preprint. Click to download.

- SupplementaryTable1.xls
- SupplementaryTable2.xls
- SupplementaryTable3.xlsx